

Cerebellar neurodegeneration in the absence of microRNAs

Anne Schaefer,¹ Dónal O'Carroll,² Chan Lek Tan,¹ Dean Hillman,^{3,4} Mutsuyuki Sugimori,⁴ Rodolfo Llinás,⁴ and Paul Greengard¹

¹Laboratory of Molecular and Cellular Neuroscience and ²Laboratory of Lymphocyte Signaling, The Rockefeller University, New York, NY 10021

³Department of Otolaryngology and ⁴Department of Physiology and Neuroscience, New York University School of Medicine, New York, NY 10016

Genome-encoded microRNAs (miRNAs) are potent regulators of gene expression. The significance of miRNAs in various biological processes has been suggested by studies showing an important role of these small RNAs in regulation of cell differentiation. However, the role of miRNAs in regulation of differentiated cell physiology is not well established. Mature neurons express a large number of distinct miRNAs, but the role of miRNAs in postmitotic neurons has not been examined. Here, we provide evidence for an essential role of miRNAs in survival of differentiated neurons. We show that conditional Purkinje cell-specific ablation of the key miRNA-generating enzyme Dicer leads to Purkinje cell death. Deficiency in Dicer is associated with progressive loss of miRNAs, followed by cerebellar degeneration and development of ataxia. The progressive neurodegeneration in the absence of Dicer raises the possibility of an involvement of miRNAs in neurodegenerative disorders.

CORRESPONDENCE

Paul Greengard:
greengard@rockefeller.edu

The recently discovered potent role of microRNAs (miRNAs) in regulation of gene and protein expression suggests an important role for these small RNAs in regulation of various physiological processes. miRNAs are ~21-nt-long noncoding RNAs that are processed from endogenously generated ~70-nt-long hairpin structures by the RNase III enzyme Dicer. The nascent miRNA is incorporated into the RNA-induced silencing complex that mediates miRNA-dependent translational suppression or, in rare cases, cleavage of respective mRNA targets (for review see references 1–3). Ablation of the miRNA-generating enzyme Dicer revealed a requirement for miRNAs in development of immune cells (4–6), skin progenitors (7), and limb outgrowth (8). The predicted role of miRNAs in regulation of mammalian cell function has been underscored by findings that show the ability of individual miRNAs to affect differentiation and function of cells of various lineages, including T cells (9) and cardiac myocytes (10, 11).

Several lines of evidence indicate the possibility of an important role of miRNAs in neuronal cells. Compared with other organs, both

mouse and human brain express an exceptionally diverse spectrum of distinct miRNAs (12–16). Furthermore, the existence of neuron-specific miRNAs argues in favor of their important role in neuronal differentiation and/or specialized functions. The involvement of miRNAs in neuronal differentiation is strongly supported by dynamic changes in miRNA expression during brain development (14, 17, 18). Moreover, the ability of neuron-specific miRNA miR-124a to suppress expression of nonneuronal genes in an *in vitro* cell system suggests an important role for miRNAs as regulators of neuronal differentiation (19). The significance of miRNAs in neuronal physiology is also suggested by data that show miRNA involvement in dendritic spine formation and neurite outgrowth *in vitro* (20, 21). In summary, although there is mounting evidence for important roles for miRNAs in neuron cell differentiation, their role in differentiated, postmitotic neurons has not been addressed.

Using Purkinje cells as a model system to analyze the role of miRNAs in postmitotic neurons, we demonstrate an essential role for miRNAs in neuronal survival. We show that inactivation of *Dicer* leads to relatively rapid disappearance of Purkinje cell-expressed miRNAs,

The online version of this article contains supplemental material.

followed by a slow degeneration of the Purkinje cells. The loss of Dicer and the decay of miRNAs have no immediate impact on Purkinje cell function as analyzed by Purkinje cell electrophysiological characteristics and animal locomotion. However, the continuous lack of miRNAs leads eventually to Purkinje cell death and ataxia. Collectively, our data suggest that miRNAs are essential for the survival of Purkinje cells and their absence leads to a slow degeneration of these cells.

RESULTS AND DISCUSSION

Dicer inactivation in differentiated Purkinje cells

The ubiquitously expressed endonuclease Dicer is essential for the generation of miRNAs (22, 23). To address the role of miRNAs in postmitotic, differentiated neurons, we used postnatal ablation of the miRNA-generating enzyme Dicer in Purkinje cells. There were several reasons for choosing Purkinje cells as a model system for the analysis of miRNA function: (a) Purkinje cells have a well-defined anatomic location and morphology; (b) these cells are easy to quantify; (c) their electrophysiological characteristics are well established; (d) changes in Purkinje cell physiology or survival lead to a characteristic functional phenotype consisting of a profound ataxia; and (e) the conditional inactivation of *loxP*-flanked gene segments in Purkinje cells could be achieved by using Purkinje cell–specific *Pcp2* promotor–driven Cre recombinase (24). Importantly, the *Pcp2* gene remains silent until the second week after birth, at which time Purkinje cells are postmitotic and have reached their final stage of differentiation.

The Purkinje cell–specific *Dicer* inactivation was achieved by Purkinje cell–specific *Pcp2* promotor–driven Cre-mediated recombination of the *Dicer* alleles modified with *loxP* sites (*Pcp2-Cre; Dicer^{fl/fl}*; references 7 and 24). To visualize Purkinje cells that express Cre at levels sufficient for *loxP* site recombination, we used a reporter system that enables enhanced GFP (eGFP) expression after Cre-mediated *loxP* recombination (25). In the absence of Cre, the eGFP gene stays dormant but becomes activated after Cre-mediated excision of the transcriptional stop cassette that separates the eGFP gene from the ubiquitously expressed Rosa26 promoter. The expression of eGFP combined with analysis of the miRNA expression was used to follow the timing and consequence of *Dicer* inactivation in Purkinje cells.

The appearance of eGFP⁺ Purkinje cells in *Pcp2-Cre; Dicer^{fl/fl}*; Gt(ROSA)26Sor;EGFP was observed around 4 wk after birth (Fig. 1, E and H), and eGFP expression was detected in the vast majority of Purkinje cells around 8 wk of age (Fig. 1, F and I). At both time points the brain-specific miRNA miR-124a, which is highly abundant in control Purkinje cells, could not be detected in Purkinje cells of *Pcp2-Cre; Dicer^{fl/fl}*; Gt(ROSA)26Sor;EGFP mice (Fig. 1, J–L). The lack of the highly abundant and widely expressed miRNA miR-124a in Purkinje cells, but not in neighboring granule cells of *Pcp2-Cre; Dicer^{fl/fl}*; Gt(ROSA)26Sor;EGFP mice, suggests efficient and Purkinje cell–specific *Dicer* inactivation at 4 wk of age.

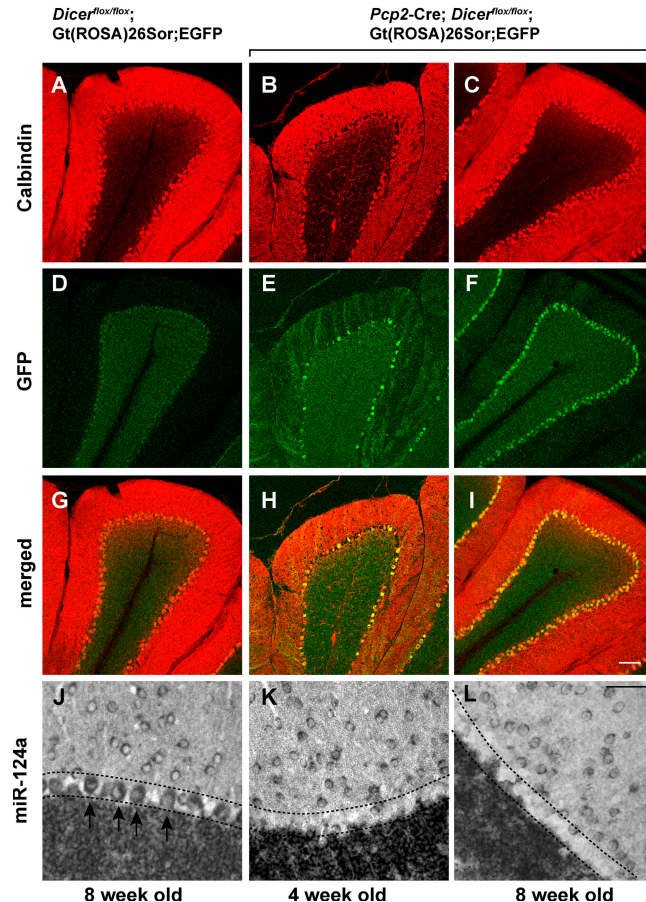


Figure 1. *Dicer* inactivation in postnatal Purkinje cells. 20- μ m-thick cerebellar sections of 8-wk-old control *Dicer*^{fl/fl}; Gt(ROSA)26Sor;EGFP (A, D, and G), and experimental *Pcp2-Cre; Dicer*^{fl/fl}; Gt(ROSA)26Sor;EGFP mice at 4 (B, E, and H) and 8 (C, F, and I) wk of age are shown. To visualize Purkinje cells, the cerebella sections were stained with anti-calbindin antibody (red). Purkinje cells expressing Cre at levels inducing *loxP* recombination were visualized by expression of eGFP using an anti-GFP antibody (green). The expression of brain-specific miRNA miR-124a in 8-wk-old control (J) and *Pcp2-Cre; Dicer*^{fl/fl}; Gt(ROSA)26Sor;EGFP mice at 4 (K) and 8 (L) wk of age was detected by *in situ* hybridization. Arrows indicate individual Purkinje cells, and the Purkinje cell layer is indicated by dashed lines. Bars: A–I, 100 μ m; J–L, 50 μ m.

Dicer deficiency alters the pattern and levels of miRNA expression in Purkinje cells

Similar to nonfractionated brain tissue (12–16), wild-type Purkinje cells express various miRNAs (Table S1, available at <http://www.jem.org/cgi/content/full/jem.20070823/DC1>). Many of these miRNAs, such as miR-101a, miR-124a, miR-125b, miR-134, miR-138 and miR-181a, have a relatively broad expression pattern and are present in neurons in numerous parts of the mouse brain. On the other hand, the miRNAs miR-9, miR-9*, miR-21, miR-23a, miR-27b, miR-34c, miR-128a, miR-128b, miR-132, miR-135, miR-136, miR-137, miR-153, miR-154, miR-211, miR-218, miR-219, miR-222, and miR-338, which are present in whole brain extracts (12–16), are not expressed in Purkinje cells (unpublished data).

As judged by *in situ* analysis of the miRNA expression, inactivation of *Dicer* had different effects on the timing of the disappearance of the Purkinje cell-expressed miRNAs. Purkinje cells of 8-wk-old *Pcp2-Cre; Dicer^{flx/flx}* mice did not express miR-1, miR-29a, miR-30c, miR-101a, miR-103, miR-124a, miR-125b, and miR-181a at detectable levels (Table S1 and Fig. 2). However, >2 mo after the first appearance of the eGFP⁺ Purkinje cells and hence well beyond the time of *Dicer* inactivation (Fig. 1), the miRNAs miR-107, miR-134, miR-138, miR-143, miR-149, miR-212, miR-221, and miR-329 remained detectable in the cerebellum of the *Pcp2-Cre; Dicer^{flx/flx}* mice (Table S1 and Fig. 2). The observed presence of miRNA in the absence of *Dicer* could be genuine and reflect differential stability of the miRNAs. Alternatively, the revealed *in situ* hybridization signals may reflect nonspecific binding of the miRNA-specific probes to the pre-miRNAs that accumulate in the absence of *Dicer*.

Deficiency in *Dicer* and miRNAs leads to degeneration of Purkinje cells

The absence of *Dicer* and the decline in miRNA expression in the cerebellum of 8-wk-old *Pcp2-Cre; Dicer^{flx/flx}* mice had no obvious effect on Purkinje cell morphology or number (Figs. 1 and 2). Similar to the control mice, the Purkinje cells of 10-wk-old *Pcp2-Cre; Dicer^{flx/flx}* mice displayed unaltered cell bodies and highly branched dendrites of normal width and length (Fig. 3, B, F, J, and M). Analysis of the electrophysiological properties of Purkinje cells of 10-wk-old *Pcp2-Cre; Dicer^{flx/flx}* mice did not reveal significant differences

between the mutant and wild-type Purkinje cells. These results indicate that there were no obvious changes in the synaptic transmission properties of the parallel or climbing fiber synapses in 10-wk-old mice. Furthermore, judging from spike waveform and repetitive firing properties, voltage-gated ionic channel distribution over the Purkinje soma dendritic plasma membrane was normal (not depicted).

Absence of miRNAs resulted eventually in Purkinje cell death and degeneration of the cerebellum (Fig. 3, C, D, G and H). Purkinje cells of the 10-wk-old *Pcp2-Cre; Dicer^{flx/flx}* mice were morphologically similar to control mice (Fig. 3, I, J, L, and M). In contrast, the dendrites of 13-wk-old mutant Purkinje cells showed spine loss in combination with fragmentation of the dendritic compartment, enlarged varicosities, and blebs in the form of pearl-like structures. Notably, all of these fragmented dendrites were still enclosed by an intact plasma membrane as determined by their ability to retain the fluorescent dye (Fig. 3, K and N).

The consequences of miRNA deficiency became particularly obvious between 13 and 17 wk of age. During this period, degenerative alterations in *Dicer*-deficient Purkinje cells spread from the anterior zone (lobules I–V) to the central (lobules VI–VII) and posterior (lobules VIII–IX) zones (Fig. 3, C and D).

At the ultrastructural level, dying Purkinje cells displayed condensation of the cytoplasm accompanied by the occurrence of intracisternal and cytosolic electron-dense structures that are reminiscent of protein inclusions, autophagic-like vacuoles, and membrane whorls (Fig. 4, A–E). In addition,

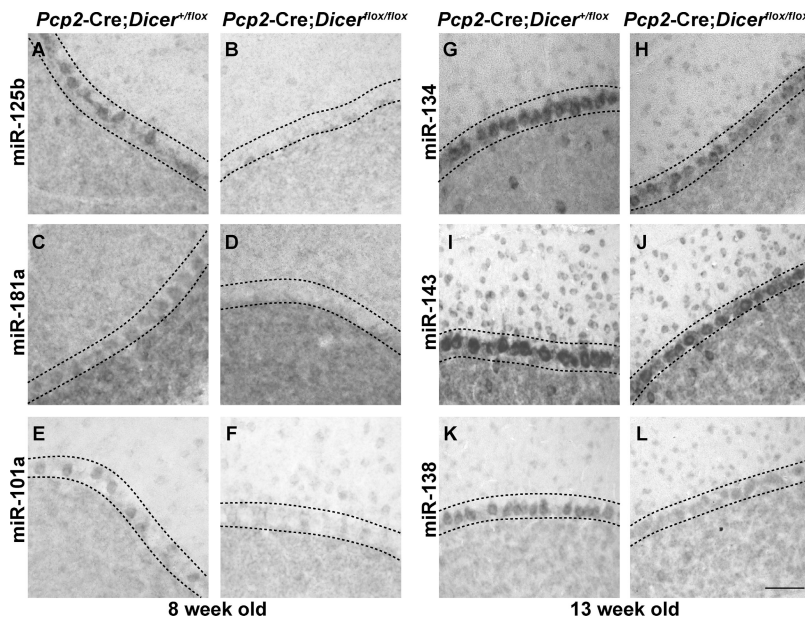


Figure 2. Expression of miRNAs in *Dicer*-deficient Purkinje cells. 12- μ m-thick cerebellar sections of 8 (A–F) or 13 (G–L) wk control *Pcp2-Cre; Dicer^{+/flx}* and experimental *Pcp2-Cre; Dicer^{flx/flx}* mice are shown. The expression of miR-125b (A and B), miR-181a (C and D), and miR-101a (E and F), representative of miRNAs that are below detection limit by 8 wk

of age, and miR-134 (G and H), miR-143 (I and J), and miR-138 (K and L), representative for miRNAs that remain detectable at 13 wk of age, were detected by *in situ* hybridization with the corresponding specific probes. Bar: A–L, 50 μ m.

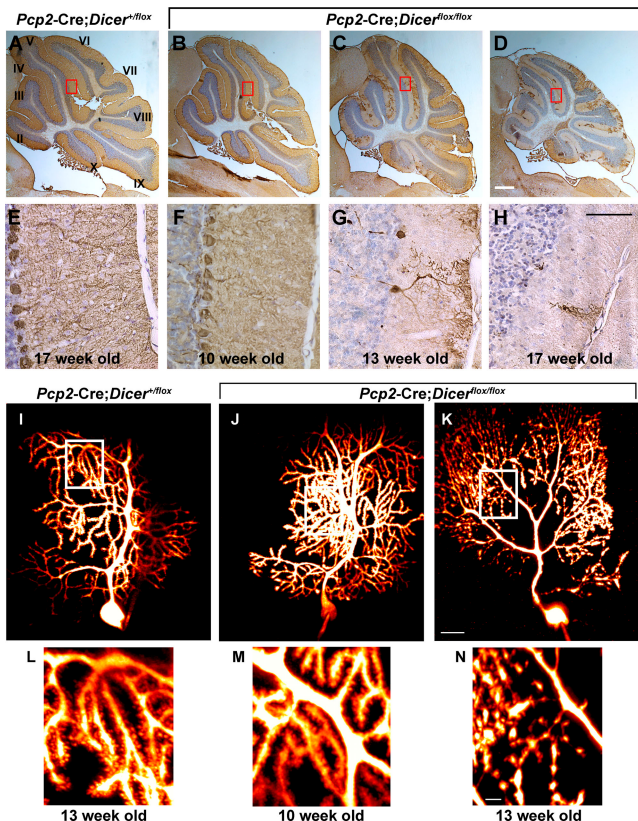


Figure 3. Postnatal inactivation of Dicer leads to cerebellar degeneration. 12- μm -thick sagittal cerebellar sections of 17-wk-old control *Pcp2-Cre; Dicer*^{+/−} mice (A and E) and 10- (B and F), 13- (C and G), and 17- (D and H) wk-old experimental *Pcp2-Cre; Dicer*^{fl/fl} mice are shown. Purkinje cells were visualized by immunohistochemistry using an antibody to calbindin (brown). Sections are counterstained using Nissl stain (blue). Cerebellar lobules are indicated by roman numerals. The sections outlined by red rectangles in A–D are amplified in E–H. Morphological changes in Dicer-deficient Purkinje cells were visualized using two-photon images after intracellular injection of the calcium-sensing dye Fura 2. 13-wk-old control *Pcp2-Cre; Dicer*^{+/−} (I and L) and 10- (J and M) and 13- (K and N) wk-old *Pcp2-Cre; Dicer*^{fl/fl} mice are shown. The individual images were stacked and visualized using Imaris software. The sections outlined by white rectangles in I–K are shown in more detail in L–N. Bars: A–D, 1 mm; E–H, 50 μm ; I–K, 20 μm ; L–N, 5 μm .

few Tdt-mediated dUTP-biotin nick-end labeling (TUNEL)⁺ and hence apoptotic nuclei cells were present in the cerebellar Purkinje cells of *Pcp2-Cre; Dicer*^{fl/fl} mice (Fig. 4, F–H), whereas many TUNEL⁺ granule cells were observed (not depicted). The apoptotic death of granule cells is likely to be induced by dying Purkinje cells as suggested by earlier findings (26, 27).

In summary, deficiency in miRNAs resulted in a slow Purkinje cell degeneration. Given the relatively global nature of the miRNA deficiency, the cause of Purkinje cell death is hard to determine. It cannot be excluded that the lack of negative regulation of protein expression by miRNAs leads to protein accumulation, followed by cell stress response and death. In support of this model, we observed accumulation of

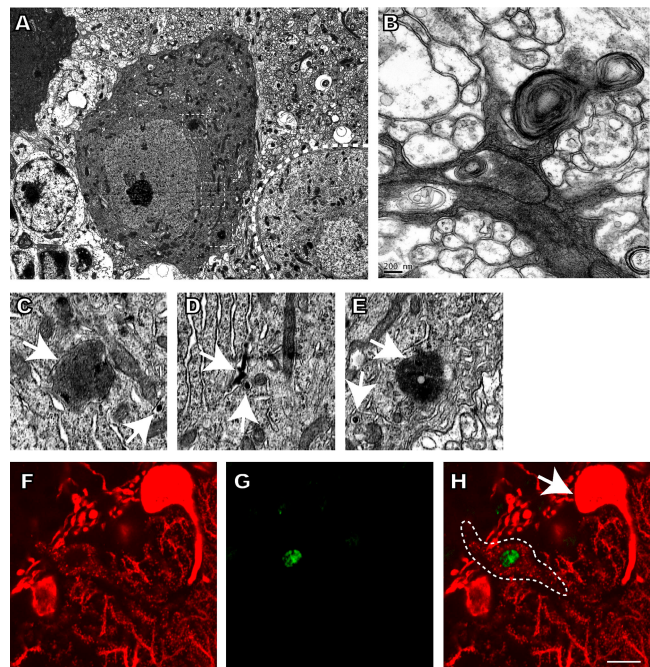


Figure 4. Purkinje cell death in *Pcp2-Cre; Dicer*^{fl/fl} mice. Electron microscopy images of degenerating Dicer-deficient Purkinje cells (A–E). Degenerating cells display condensation of the cytoplasm in cell bodies (A) and the dendritic compartment (B). Cytoplasmic condensation is associated with the occurrence of protein accumulations (A), autophagic vacuoles, and membrane whorls (B). Region of interests in A are marked by squares and shown in more detail (C–E). Membranes surrounding protein accumulations (C and E) and intracisternal inclusions (C–E) are indicated by arrows. The 12- μm -thick cerebellar section of a 13-wk-old *Pcp2-Cre; Dicer*^{fl/fl} mouse is shown in F–H. Purkinje cells were visualized using anti-calbindin antibody (red), and apoptotic cells were detected by TUNEL staining (green). A TUNEL⁺ degenerating Purkinje cell (indicated by a dashed line) can be seen close to a TUNEL[−] normal-appearing Purkinje cell (arrow). Bars: A, 5 μm ; B, 0.2 μm ; C–E, 1 μm ; F–H, 10 μm .

intracisternal and cytosolic protein aggregates in Dicer-deficient Purkinje cells (Fig. 4, A–E). It is also possible that the lack of pre-miRNA processing in the absence of Dicer results in accumulation of pre-miRNAs at toxic quantities.

Dicer deficiency in Purkinje cells causes ataxia

The depletion of miRNAs and accompanying degeneration of Purkinje cells led to ataxia. The motor functions of young (8-wk-old) *Pcp2-Cre; Dicer*^{fl/fl} mice were indistinguishable from those of control mice. However, at 13 wk of age and at the time of significant miRNA decline, the *Pcp2-Cre; Dicer*^{fl/fl} mice started to develop a slight tremor and mild ataxia. These symptoms were aggravated within the next months. The analysis of motor function and balance, as examined by the rotarod test, displayed a severe impairment in 17-wk-old *Pcp2-Cre; Dicer*^{fl/fl} mice (Fig. 5 A). The footprint analysis confirmed an ataxic walking pattern of the *Pcp2-Cre; Dicer*^{fl/fl} mice (Fig. 5 B). These results indicate that miRNA deficiency in Purkinje cells results in a severe cerebellar dysfunction around 17 wk of age.

Conclusion

Here, we show the essential role of Dicer and miRNAs in the regulation of postmitotic neuronal survival. Although Dicer deficiency had no immediate impact on Purkinje cell function, the long-term absence of Dicer resulted in a neurodegenerative process. This pattern of Purkinje cell degeneration in the absence of miRNAs bears obvious similarity to processes associated with the slow progressing neurodegenerative diseases such as Alzheimer's and Parkinson's disease. Our findings may help to identify individual miRNAs that contribute critically to neuronal cell survival. Finally, identification of miRNAs as critical regulators of neuronal survival may provide additional insight into the molecular mechanisms of neurodegeneration.

MATERIALS AND METHODS

Mice. *Dicer*^{flox/flox} (7), *Pcp2-Cre* (24), and Gt(ROSA)26Sor;EGFP (25) mice were intercrossed to generate *Pcp2-Cre; Dicer*^{flox/flox} and *Pcp2-Cre; Dicer*^{+/flox}; Gt(ROSA)26Sor;EGFP mice. Genotyping was performed as described previously (7, 24, 25). Mice were housed under standard laboratory conditions at The Rockefeller University Laboratory Animal Research Center. Protocols were approved by The Rockefeller University Institutional Animal Care and Use Committee.

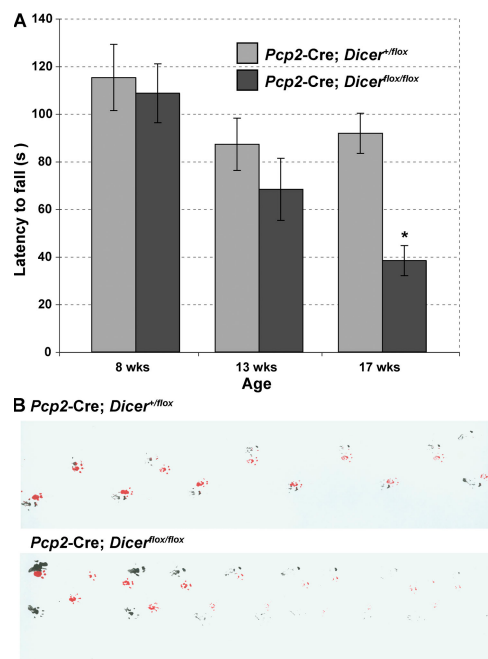


Figure 5. Dicer deficiency in Purkinje cells causes ataxia. (A) Rotarod test on *Pcp2-Cre; Dicer*^{flox/flox} mice compared with their littermate controls. Statistical analysis was performed using Anova single factor analysis ($F = 5.976822099$; $P = 0.00024395$; $F_{crit} = 2.41735603$). Latency to fall from the rod was measured in control *Pcp2-Cre; Dicer*^{+/flox} (gray) and mutant *Pcp2-Cre; Dicer*^{flox/flox} (black) mice at 8 (control, $n = 10$; mutant, $n = 8$; $P = 0.73494913$), 13 (control, $n = 10$; mutant, $n = 7$; $P = 0.28503378$), and 17 (control, $n = 9$; mutant, $n = 8$; $P = 0.00016573$) wk of age. Results are expressed as means, and error bars represent \pm SEM. p-values are from the unpaired two-tailed Student's *t* test. (B) Footprint analysis. Footprints of 17-wk-old male control and *Pcp2-Cre; Dicer*^{flox/flox} mice are shown. The mutant animal exhibits a wide-based ataxic gait. Red, front paws; black, hind paws.

Cerebellar slice preparation. Mice were anesthetized with pentobarbital and transcardially perfused as described previously (28). Brains were post-fixed with 4% paraformaldehyde, incubated sequentially in 5, 15, and 30% wt/vol sucrose in PBS at 4°C, and embedded in Neg-50 medium (Richard Allen Scientific). 10–20- μ m-thick sagittal sections were mounted on Superfrost/Plus slides (Fisher Scientific). Before use, sections were thawed, dried for 10 min at room temperature, and washed in PBS.

miRNA detection. MiRNAs were detected by *in situ* hybridization using 3' DIG-labeled LNA oligonucleotide probes from Exiqon purified using Sephadex G25 MicroSpin columns (GE Healthcare). 1–10 pmol of each labeled probe was used in 250 μ l of hybridization buffer per slide. Hybridization was performed according to the published protocol (29).

Immunohistochemistry and indirect immunofluorescence. Sections were incubated in 0.3% H₂O₂/PBS at room temperature for 30 min, permeabilized with 0.2% Triton/PBS, and blocked with 2% normal goat serum. Sections were incubated overnight at 4°C with a primary antibody against calbindin D-28 (dilution 1:5000; Swant) and visualized by the avidin-biotin-peroxidase complex method (Vector Laboratories). The sections were counterstained using standard Nissl-stain. For indirect immunofluorescence analysis, calbindin D-28 (dilution 1:5000; Swant) and GFP (dilution 1:5,000; ab6556; Abcam) antibodies followed by incubation with Alexa Fluor 546/488-labeled goat anti-mouse/anti-rabbit IgGs (H+L) (dilution 1:500; Invitrogen) were used.

TUNEL staining. The In Situ Cell Death Detection kit (fluorescein; Roche) was used according to the manufacturer's instructions. Purkinje cells were visualized by subsequent immunostaining using an antibody against calbindin D-28 (as described above).

All sections from *in situ*, immunohistochemistry, immunofluorescence, and TUNEL staining were then visualized on a confocal microscope (LSM510; Carl Zeiss MicroImaging, Inc.).

Behavioral analysis. The motor function and balance of control and *Pcp2-Cre; Dicer*^{flox/flox} mice were analyzed via the rotarod task (Economex Rotarod; Columbus Instruments) at initial rotation of 1 rpm, accelerating at a rate of 0.3 rpm/sec. The time taken for the mice to fall from the rod was measured in seconds. If a mouse stayed on the rod until the end of the 3-min trial, a time of 180 s was recorded. Mice were subjected to 5 d of consecutive trials, and measurements were taken on day 6. Statistical analysis was performed using Student's *t* test and Anova single factor analysis.

Footprint patterns were obtained by dipping front paws in red nontoxic ink and hind paws in black nontoxic ink and placing mice at one end of a dark tunnel.

Electron microscopy. Mice were perfused using 5 ml PBS followed by 50 ml 2.5% glutaraldehyde in 0.1 M cacodylate acid buffer, pH 7.4, and processed for transmission electron microscopy according to standard protocols.

Two-photon imaging. Imaging was implemented with 100 μ M of the calcium-sensing dye Fura 2 dissolved in the patch electrode solution. The images were obtained using a two-photon laser microscope (AX70; Olympus) as described previously (30). Two-photon images were acquired and processed with an in-house program. Imaris software was used for visualization and analysis of the individual images.

Online supplemental material. In Table S1, expression of miRNAs in Dicer-deficient Purkinje cells is shown. The expression of many miRNAs reported for whole brain extracts (12–16) has been validated for Purkinje cells using *in situ* hybridization in 8-wk-old C57BL/6 wild-type mice. The expression levels of these miRNAs in Purkinje cells of 8- and 13-wk-old *Pcp2-Cre; Dicer*^{flox/flox} mice relative to control *Pcp2-Cre; Dicer*^{+/flox} mice are given. The expression levels of miRNAs in control mice were given an arbitrary value of “++.” The miRNA expression in Purkinje cells of

Pcp2-Cre; Dicer^{flx/flx} mice is indicated as follows: +++, strong; ++, medium; +, weak; −, absent. Table S1 is available at <http://www.jem.org/cgi/content/full/jem.20070823/DC1>.

We would like to thank Helen Shio for electron microscopy, Adam Intrator for his excellent technical help, and Elizabeth Griggs for her help in the preparation of the figures. We would like to thank Dr. Myriam Heiman, Dr. Fekrije Selimi, and Dr. Alexander Tarakhovsky for helpful discussions.

This work was supported in part by National Institutes of Health grants MH074866, DA10044, and AG09464 (to P. Greengard); the Dr. Miriam and Sheldon G. Adelson Medical Research Foundation (to P. Greengard and A. Schaefer); and National Institutes of Health grant NS13742 (to R. Llinás). A. Schaefer is a recipient of a Deutsche Forschungsgemeinschaft postdoctoral fellowship (SCHA 1482/1-1). D. O'Carroll was a National Genetics Foundation Fellow of the Irvington Institute for Immunological Research and acknowledges their support.

The authors have no conflicting financial interests.

Submitted: 24 April 2007

Accepted: 5 June 2007

REFERENCES

1. Ambros, V. 2004. The functions of animal microRNAs. *Nature*. 431:350–355.
2. Bartel, D.P. 2004. MicroRNAs: genomics, biogenesis, mechanism, and function. *Cell*. 116:281–297.
3. He, L., and G.J. Hannon. 2004. MicroRNAs: small RNAs with a big role in gene regulation. *Nat. Rev. Genet.* 5:522–531.
4. Cobb, B.S., T.B. Nesterova, E. Thompson, A. Hertweck, E. O'Connor, J. Godwin, C.B. Wilson, N. Brockdorff, A.G. Fisher, S.T. Smale, and M. Merkenschlager. 2005. T cell lineage choice and differentiation in the absence of the RNase III enzyme Dicer. *J. Exp. Med.* 201: 1367–1373.
5. Cobb, B.S., A. Hertweck, J. Smith, E. O'Connor, D. Graf, T. Cook, S.T. Smale, S. Sakaguchi, F.J. Livesey, A.G. Fisher, and M. Merkenschlager. 2006. A role for Dicer in immune regulation. *J. Exp. Med.* 203:2519–2527.
6. Muljo, S.A., K.M. Ansel, C. Kanellopoulou, D.M. Livingston, A. Rao, and K. Rajewsky. 2005. Aberrant T cell differentiation in the absence of Dicer. *J. Exp. Med.* 202:261–269.
7. Yi, R., D. O'Carroll, H.A. Pasolli, Z. Zhang, F.S. Dietrich, A. Tarakhovsky, and E. Fuchs. 2006. Morphogenesis in skin is governed by discrete sets of differentially expressed microRNAs. *Nat. Genet.* 38: 356–362.
8. Harfe, B.D., M.T. McManus, J.H. Mansfield, E. Hornstein, and C.J. Tabin. 2005. The RNaseIII enzyme Dicer is required for morphogenesis but not patterning of the vertebrate limb. *Proc. Natl. Acad. Sci. USA*. 102:10898–10903.
9. Li, Q.J., J. Chau, P.J. Ebert, G. Sylvester, H. Min, G. Liu, R. Braich, M. Manoharan, J. Soutschek, P. Skare, et al. 2007. miR-181a is an intrinsic modulator of T cell sensitivity and selection. *Cell*. 129:147–161.
10. Zhao, Y., J.F. Ransom, A. Li, V. Vedantham, M. von Drehle, A.N. Muth, T. Tsuchihashi, M.T. McManus, R.J. Schwartz, and D. Srivastava. 2007. Dysregulation of cardiogenesis, cardiac conduction, and cell cycle in mice lacking miRNA-1-2. *Cell*. 129:303–317.
11. van Rooij, E., L.B. Sutherland, X. Qi, J.A. Richardson, J. Hill, and E.N. Olson. 2007. Control of stress-dependent cardiac growth and gene expression by a microRNA. *Science*. 316:575–579.
12. Babak, T., W. Zhang, Q. Morris, B.J. Blencowe, and T.R. Hughes. 2004. Probing microRNAs with microarrays: tissue specificity and functional inference. *RNA*. 10:1813–1819.
13. Barad, O., E. Meiri, A. Avniel, R. Aharonov, A. Barzilai, I. Bentwich, U. Einav, S. Gilad, P. Hurban, Y. Karov, et al. 2004. MicroRNA expression detected by oligonucleotide microarrays: system establishment and expression profiling in human tissues. *Genome Res.* 14:2486–2494.
14. Miska, E.A., E. Alvarez-Saavedra, M. Townsend, A. Yoshii, N. Sestan, P. Rakic, M. Constantine-Paton, and H.R. Horvitz. 2004. Microarray analysis of microRNA expression in the developing mammalian brain. *Genome Biol.* 5:R68.
15. Sempere, L.F., S. Freemantle, I. Pitha-Rowe, E. Moss, E. Dmitrovsky, and V. Ambros. 2004. Expression profiling of mammalian microRNAs uncovers a subset of brain-expressed microRNAs with possible roles in murine and human neuronal differentiation. *Genome Biol.* 5:R13.
16. Lagos-Quintana, M., R. Rauhut, A. Yalcin, J. Meyer, W. Lendeckel, and T. Tuschl. 2002. Identification of tissue-specific microRNAs from mouse. *Curr. Biol.* 12:735–739.
17. Krichevsky, A.M., K.S. King, C.P. Donahue, K. Khrapko, and K.S. Kosik. 2003. A microRNA array reveals extensive regulation of microRNAs during brain development. *RNA*. 9:1274–1281.
18. Smirnova, L., A. Grafe, A. Seiler, S. Schumacher, R. Nitsch, and F.G. Wulczyn. 2005. Regulation of miRNA expression during neural cell specification. *Eur. J. Neurosci.* 21:1469–1477.
19. Lim, L.P., N.C. Lau, P. Garrett-Engele, A. Grimson, J.M. Schelter, J. Castle, D.P. Bartel, P.S. Linsley, and J.M. Johnson. 2005. Microarray analysis shows that some microRNAs downregulate large numbers of target mRNAs. *Nature*. 433:769–773.
20. Vo, N., M.E. Klein, O. Varlamova, D.M. Keller, T. Yamamoto, R.H. Goodman, and S. Impey. 2005. A cAMP-response element binding protein-induced microRNA regulates neuronal morphogenesis. *Proc. Natl. Acad. Sci. USA*. 102:16426–16431.
21. Schrott, G.M., F. Tuebing, E.A. Nigh, C.G. Kane, M.E. Sabatini, M. Kiebler, and M.E. Greenberg. 2006. A brain-specific microRNA regulates dendritic spine development. *Nature*. 439:283–289.
22. Bernstein, E., A.A. Caudy, S.M. Hammond, and G.J. Hannon. 2001. Role for a bidentate ribonuclease in the initiation step of RNA interference. *Nature*. 409:363–366.
23. Bernstein, E., S.Y. Kim, M.A. Carmell, E.P. Murchison, H. Alcorn, M.Z. Li, A.A. Mills, S.J. Elledge, K.V. Anderson, and G.J. Hannon. 2003. Dicer is essential for mouse development. *Nat. Genet.* 35:215–217.
24. Zhang, X.M., A.H. Ng, J.A. Tanner, W.T. Wu, N.G. Copeland, N.A. Jenkins, and J.D. Huang. 2004. Highly restricted expression of Cre recombinase in cerebellar Purkinje cells. *Genesis*. 40:45–51.
25. Mao, X., Y. Fujiwara, A. Chapdelaine, H. Yang, and S.H. Orkin. 2001. Activation of EGFP expression by Cre-mediated excision in a new ROSA26 reporter mouse strain. *Blood*. 97:324–326.
26. Wetts, R., and K. Herrup. 1983. Direct correlation between Purkinje and granule cell number in the cerebella of lurcher chimeras and wild-type mice. *Brain Res.* 312:41–47.
27. Caddy, K.W., and T.J. Biscoe. 1979. Structural and quantitative studies on the normal C3H and Lurker mutant mouse. *Philos. Trans. R. Soc. Lond. B Biol. Sci.* 287:167–201.
28. Lee, K.W., Y. Kim, A.M. Kim, K. Helmin, A.C. Nairn, and P. Greengard. 2006. Cocaine-induced dendritic spine formation in D1 and D2 dopamine receptor-containing medium spiny neurons in nucleus accumbens. *Proc. Natl. Acad. Sci. USA*. 103:3399–3404.
29. Kloosterman, W.P., E. Wienholds, E. de Bruijn, S. Kauppinen, and R.H. Plasterk. 2006. In situ detection of miRNAs in animal embryos using LNA-modified oligonucleotide probes. *Nat. Methods*. 3:27–29.
30. Hirata, K., M. Nakagawa, F.J. Urbano, M.D. Rosato-Siri, J.E. Moreira, O.D. Uchitel, M. Sugimori, and R. Llinás. 1999. Reduced facilitation and vesicular uptake in crustacean and mammalian neuromuscular junction by T-588, a neuroprotective compound. *Proc. Natl. Acad. Sci. USA*. 96:14588–14593.